PACS & SPIRE photometer maps of M33: First results of the Herschel M33 extended survey (HERM33ES)

C.Kramer[1], C.Buchbender[1], E.M.Xilouris[2], M.Boquien[3], J.Braine[4], D.Calzetti[4], S.Lord[5], B.Mookerjea[6], G.Quintana-Lacaci[1], M.Relano[7], G.Stacey[8], F.S.Tabatabaei[9], S.Verley[10], S.Aalto[11], S.Akras[2], M.Albrecht[12], S.Anderl[12], R.Beck[9], F.Bertoldi[12], F.Combes[13], M.Dumke[14], S.Garcia-Burillo[15], M.Gonzalez[1], P.Gratier[4], R.Güsten[9], C.Henkel[9], F.P.Israel[16], B.Koribalski[17], A.Lundgren[14], J.Martin-Pintado[18], M.Rollig[19], E.Rosolowsky[20], K.Schuster[21], K.Sheth[22], A.Sievers[1], J.Stutzki[19], R.P.J.Tilanus[23], F.van der Tak[24], P.van der Werf[16], M.C.Wiedner[13]

[1] IRAM, Granada, Spain, [2]National Observatory of Athens, Greece, [3] University of Massachusetts, USA, [4] Laboratoire d'Astrophysique de Bordeaux, France, [5] IPAC, Pasadena, USA [6] Tata Institute of Fundamental Research, Mumbai, India, [7] University of Cambridge, UK, [8] Cornell University, USA, [9] MPIfR, Bonn, Germany, [10] Universidad de Granada, Spain, [11] Onsala Observatory, Sweden, [12]Argelander Institut fur Astronomie, Germany, [13] Observatoire de Paris, France, [14] ESO, Santiago, Chile, [15] OAN, Madrid, Spain, [16] Leiden Observatory, The Netherlands, [17] ATNF, CSIRO, Epping, Australia, [18] CSIC, Madrid, Spain, [19] I. Physikalisches Institut, Universitat zu Koln, Germany, [20]University of British Columbia, Canada, [21] IRAM, Grenoble, France, [22] California Institute of Technology, USA, [23]JAC, Hilo, USA, [24]SRON, Groningen, The Netherlands

Abstract

Within the framework of the Herschel open time key project HERM33ES, we are studying the star forming interstellar medium in the nearby, metal-poor spiral galaxy M33, exploiting the high resolution and sensitivity of Herschel.

We use PACS and SPIRE maps at 100, 160, 250, 350, and 500μm wavelength, to study the variation of the spectral energy distributions (SEDs) with galacto-centric distance (Kramer et al. 2010).

Detailed SED modeling is performed using azimuthally averaged fluxes in elliptical rings of 2kpc width, out to 8kpc galacto-centric distance. Simple isothermal and two-component grey body models, with fixed dust emissivity index, are fitted to the SEDs between 24μm and 500μm using also MIPS/Spitzer data, to derive first estimates of the dust physical conditions.

The far-infrared and submillimeter maps reveal the branched, knotted spiral structure of M33. An underlying diffuse disk is seen in all SPIRE maps (250-500μm). Two component fits to the SEDs agree better than isothermal models with the observed, total and radially averaged flux densities. The two component model, with β fixed at 1.5, best fits the global and the radial SEDs. The cold dust component clearly dominates; the relative mass of the warm component is less than 0.3% for all the fits. The temperature of the warm component is not well constrained and is found to be about 60K. The temperature of the cold component drops significantly from ~24K in the inner 2kpc radius to 13K beyond 6kpc radial distance, for the best fitting model. The gas-to-dust ratio, averaged over the galaxy, is higher than the solar value by a factor of 1.5 and is roughly in agreement with the subsolar metallicity of M33.

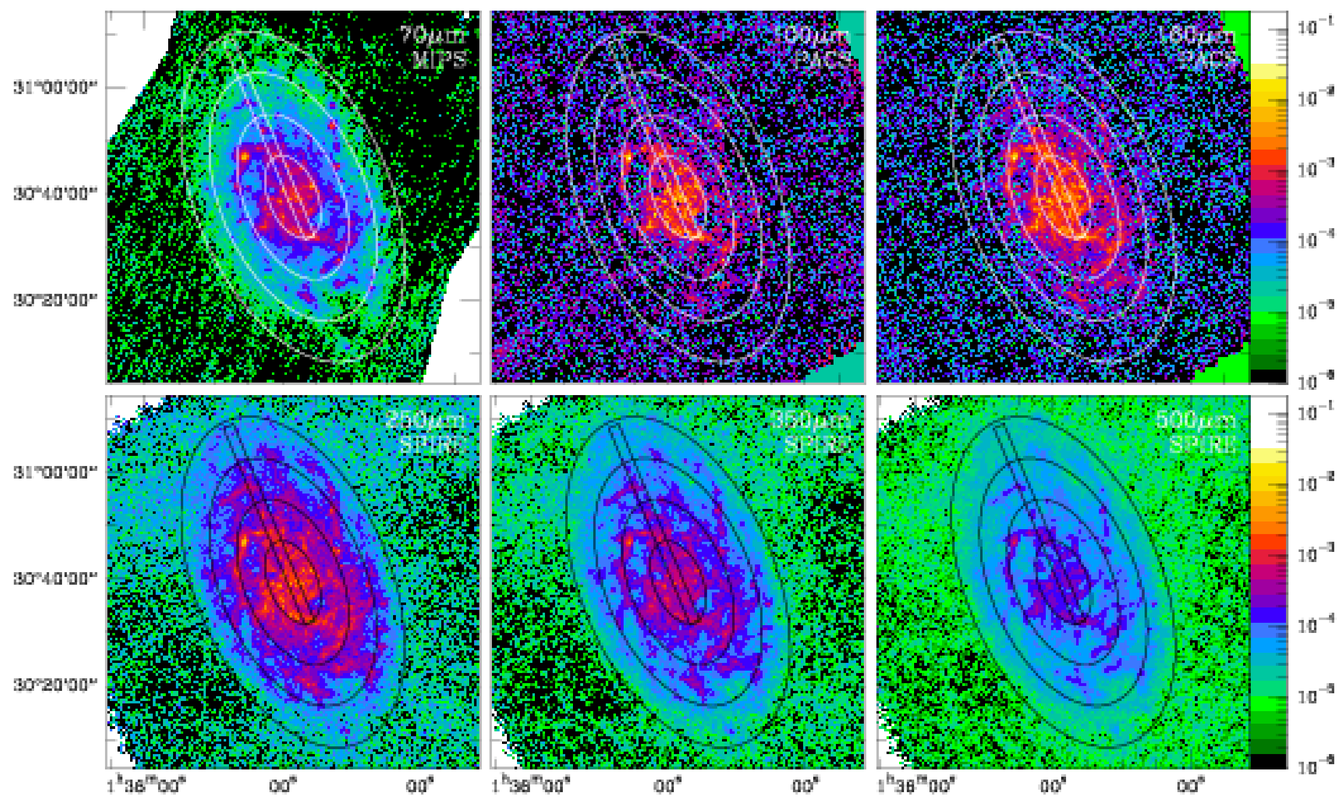

Figure 1. Maps of FIR and submillimeter emission of M33 covering a region of 70'x70' centered on 01:33:51.02 30:39:36.7 (J2000). **Upper:** MIPS/Spitzer 70μm map (Tabatabaei et al. 2007) and PACS/Herschel maps at 100μm and 160μm. **Lower:** SPIRE/Herschel maps at 250, 350, and 500μm. All data are on the Jy/arcsec^2 scale and at their nominal resolutions. Ellipses denote 2, 4, 6, 8kpc galacto-centric distances with inclination 56deg and position angle 22.5deg. The rectangle delineates the 2'x40' wide strip along the major axis, which will be mapped with HIFI and PACS in spectroscopy mode. A large number of distinct sources delineates the spiral arms. Their properties are studied by Verley et al. (2010) and Boquien et al. (2010).

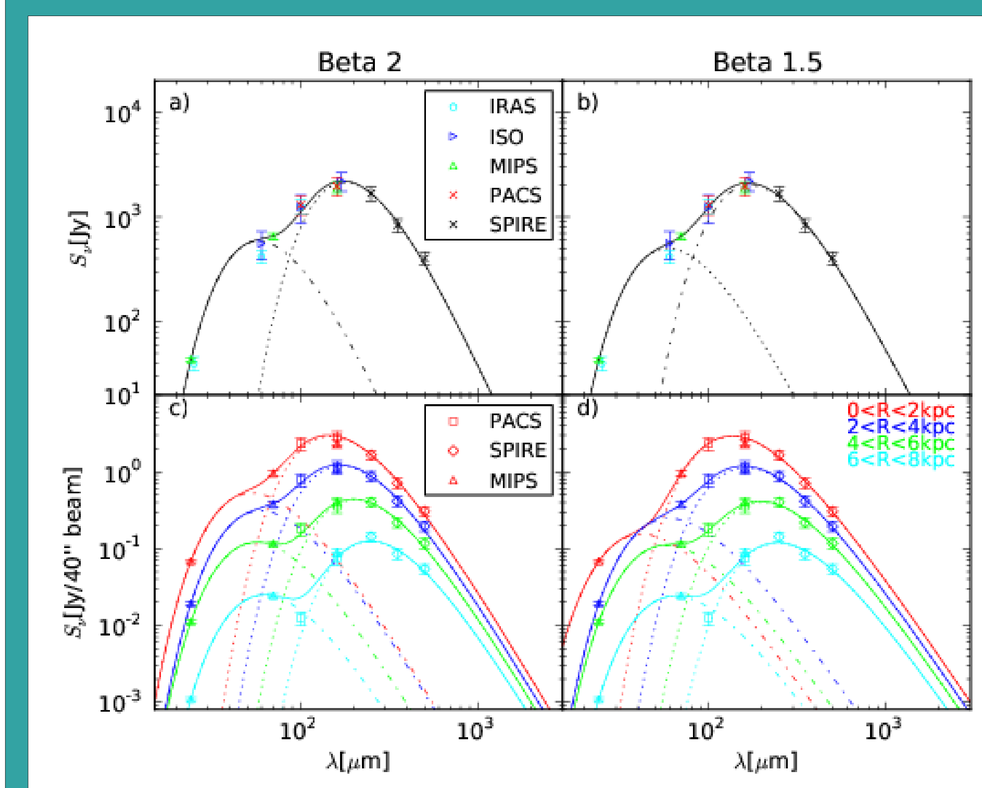

Figure 2. SEDs of M33 at wavelengths between 24μm and 500mm. **a,b:** Total integrated SED of M33, combining data of PACS & SPIRE, with data of MIPS/Spitzer, ISOCAM, and IRAS. **c, d:** Radially averaged SEDs in zones of 2kpc width. Here, we show the MIPS, PACS, and SPIRE data. **a, c:** Drawn lines show two-component grey body model fit results. The 100μm PACS flux density, measured in the outermost zone, was not used for the fits. The dust emissivity index was set to β=2. **b, d:** Drawn lines show two-component models for β=1.5.

Table 1. Results of fits of one and two emission components to the measured spectral energy distributions (SEDs) of the MIPS, PACS, SPIRE data of M33 shown in Figure 3. For the two-component fits, the dust emissivity index was kept fixed. T_c, T_w are the temperatures of the cold and warm component. M_c is the total cold dust mass per annulus. M_c/M_w is the dust mass ratio of both components. The 100 μm flux density measured in the outermost zone was not used for the fits. The columns give the radial annuli: Total: $0 < R < 8$ kpc, (1): $0 < R < 2$ kpc, (2): $2 < R < 4$ kpc, (3): $4 < R < 6$ kpc, (4): $6 < R < 8$ kpc. The last line at the bottom of the table gives the total gas masses $M_{\rm gas} = 1.36\,(M({\rm H_2}) + M({\rm H\,I}))$ (Gratier et al. 2010).

	Total	(1)	(2)	(3)	(4)
Isothermal fits					
T/[K]	29	25	28	105	37
β	0.5	1.4	0.8	−1.8	−0.8
χ^2	134	133	134	10	12
Two-component fits with $\beta = 2$					
T_c/[K]	16	20	17	14	12
T_w/[K]	50	55	49	52	47
M_c/[10^6 M$_\odot$]	8.0	1.0	2.4	3.5	4.1
M_c/M_w	1000	900	700	2200	5100
χ^2	0.8	0.5	0.6	0.9	1.8
Two-component fits with $\beta = 1.5$					
T_c/[K]	19	24	20	16	13
T_w/[K]	55	77	54	56	50
M_c/[10^6 M$_\odot$]	10	1.2	3.0	4.5	4.9
M_c/M_w	500	3800	400	1000	2000
χ^2	0.28	0.20	0.23	0.41	1.8
$M_{\rm gas}/M_c$	202	196	144	124	160
Two-component fits with $\beta = 1$					
T_c/[K]	23	28	24	19	15
T_w/[K]	62	-	64	62	54
M_c/[10^6 M$_\odot$]	12	1.6	3.6	5.7	5.9
M_c/M_w	300	-	360	440	800
χ^2	0.43	1.18	0.52	0.58	2.41
Total gas mass					
$M_{\rm gas}$/[10^8 M$_\odot$]	20.2	2.3	4.4	5.6	7.9

The cold dust component dominates the mass for the galaxy for all annuli. It drops significantly from about 24K in the inner 2kpc radius to 13K beyond 6kpc radial distance, using the two-component grey body model with β=1.5.

Table 1 gives the total gas masses Mgas of the entire galaxy, and of the elliptical annuli. These are calculated from HI and CO data presented in Gratier et al. (2010). The gas-to-dust mass ratio for the entire galaxy, using the best fitting dust model, is ~200, about a factor of 1.5 higher than the solar value of 137 (Draine et al. 2007), and a factor of 2 higher than recent dust models for the Milky Way (Weingartner & Draine 2001). A factor of about 2 is expected, as the metallicity is about half solar (Magrini et al. 2009). The gas-to-dust ratio varies between 200 and 120 in the annuli, showing no rise, as expected from the very shallow O/H abundance gradient found by Magrini et al. (2009). The gas-to-dust ratios found in M33 are similar to the typical values found in nearby galaxies (Draine et al. 2007, Bendo et al. 2010). Braine et al. (2010) combine the dust and gas data of M33 to study the gas-to-dust ratios in more detail and derive dust cross sections.

Acknowledgements: We would like to thank all those who helped us processing the PACS and SPIRE data. In particular we would like to acknowledge support from Pierre Royer, Bruno Altieri, Pat Morris, Bidushi Bhattacharya, Marc Sauvage, Michael Pohlen, Pierre Chanial, George Bendo.